

Supported Lipid Bilayer Formation: Beyond Vesicle Fusion

Joshua A. Jackman and Nam-Joon Cho*

Cite This: *Langmuir* 2020, 36, 1387–1400

Read Online

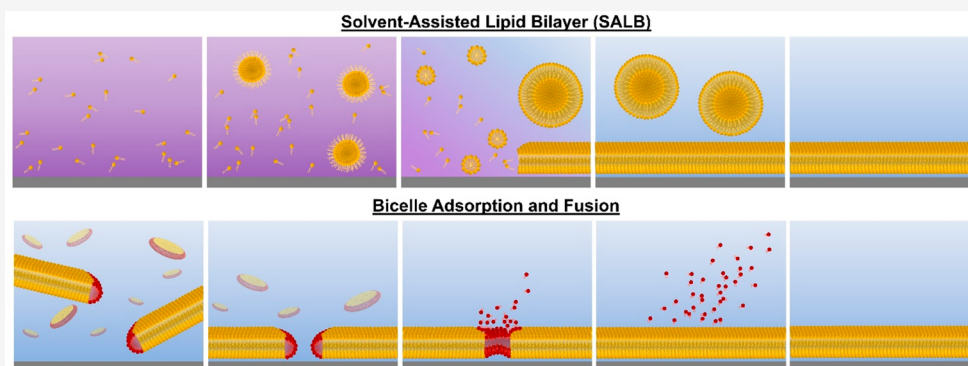
ACCESS |



Metrics & More



Article Recommendations



ABSTRACT: Supported lipid bilayers (SLBs) are cell-membrane-mimicking platforms that can be formed on solid surfaces and integrated with a wide range of surface-sensitive measurement techniques. SLBs are useful for unravelling details of fundamental membrane biology and biophysics as well as for various medical, biotechnology, and environmental science applications. Thus, there is high interest in developing simple and robust methods to fabricate SLBs. Currently, vesicle fusion is a popular method to form SLBs and involves the adsorption and spontaneous rupture of lipid vesicles on a solid surface. However, successful vesicle fusion depends on high-quality vesicle preparation, and it typically works with a narrow range of material supports and lipid compositions. In this Feature Article, we summarize current progress in developing two new SLB fabrication techniques termed the solvent-assisted lipid bilayer (SALB) and bicelle methods, which have compelling advantages such as simple sample preparation and compatibility with a wide range of material supports and lipid compositions. The molecular self-assembly principles underpinning the two strategies and important experimental parameters are critically discussed, and recent application examples are presented. Looking forward, we envision that these emerging SLB fabrication strategies can be widely adopted by specialists and nonspecialists alike, paving the way to enriching our understanding of lipid membrane properties and realizing new application possibilities.

INTRODUCTION

Phospholipid membranes are critical architectural features of biological systems across multiple length scales ranging from cells to biological nanoparticles such as exosomes and viruses.^{1–3} Biological membranes have numerous important functions including structural integrity, signaling pathways, and chemical compartmentalization.^{4–6} Thus, there has long been extensive interest in understanding the molecular design principles behind phospholipid membranes^{7,8} and developing engineered versions that can be useful for various applications such as biosensors, biocompatible coatings, and bioanalytical tools.^{9–13}

Supported lipid bilayers (SLBs) are one of the most promising model systems and are two-dimensional thin film coatings composed of a single phospholipid bilayer that is conformally attached to an underlying solid surface.^{14–18} A key advantage of SLBs is that they are compatible with a wide range of surface-sensitive measurement techniques, including acoustic, optical, plasmonic, and electrochemical sensors along with

fluorescence and atomic force microscopy techniques among many possible options.^{19–23} Depending on the measurement technique and application purpose, it is important to fabricate high-quality SLBs on target solid surfaces with advantageous properties and to also have control over the lipid composition. These design needs have motivated scientific researchers to develop many different SLB fabrication methods over the years.²⁴

Currently, the vesicle fusion method is the most widely used one to fabricate SLBs and involves the adsorption and spontaneous rupture of lipid vesicles on a target surface.^{25–28} If there are attractive interactions between a contacting vesicle and a solid surface (e.g., van der Waals and electrostatic forces),

Received: December 2, 2019

Revised: January 25, 2020

Published: January 28, 2020

then the vesicle will adsorb onto the surface.^{29,30} Depending on the vesicle–substrate interaction strength, an adsorbed vesicle can become deformed and will either remain intact or eventually rupture due to a combination of vesicle–substrate and/or vesicle–vesicle interactions.^{31–33} While vesicle fusion has proven to be useful for fabricating SLBs on silica-based surfaces, it can be a challenging technique to master, and there are numerous experimental parameters that affect SLB formation success. Key factors include vesicle properties such as lipid composition,³⁴ lipid concentration,³⁵ phase state,³⁶ size,³⁷ lamellarity,³⁸ and osmotic pressure;³⁹ solid surface properties such as atomic composition,⁴⁰ morphology,⁴¹ and nanotopography;⁴² and environmental conditions such as ionic strength,⁴³ ions,⁴⁴ temperature,⁴⁵ and solution pH.⁴⁶ Moreover, vesicle fusion works only on a narrow range of solid surfaces, while vesicles typically adsorb but remain intact on industrially useful surfaces such as gold⁴⁷ and titanium oxide.⁴⁸ To what extent the material-surface-dependent nature of SLB formation success relates to the atomic composition of the solid surface versus fabrication- and processing-related material properties such as surface roughness and functional group density remains an active area of investigation. For example, it has been demonstrated that vesicle fusion can lead to SLB formation on smooth, single-crystal gold surfaces^{49–51} as well as on single-crystal titanium oxide surfaces after wet treatment and thermal annealing in the latter case.⁵²

Additionally, when working with more biomimetic membrane compositions containing cholesterol and/or biologically important anionic lipids, optimization of the experimental conditions used with the vesicle fusion method is often necessary to achieve successful SLB fabrication. To this end, progress has been made with cholesterol-containing lipid compositions,^{53,54} natural cell membrane extracts,^{55–57} and extracellular vesicle membranes⁵⁸ as well as by using vesicle-rupturing peptide agents to form SLBs, although the latter approach requires multistep protocols and additional reagents.^{59–62} In addition, other SLB fabrication options include lipid spreading, which involves the hydration wetting of phospholipid molecules on part of a solid surface,^{63–65} along with freezing and thawing of a surface that contains already-adsorbed, intact vesicles to induce SLB formation.⁶⁶ Nevertheless, there remains ample room for improvement in terms of developing new SLB fabrication strategies that are simple and scalable and work with a wide range of solid surfaces and lipid compositions.

In this Feature Article, we introduce our recent efforts to develop the solvent-assisted lipid bilayer (SALB) and bicelle methods for SLB fabrication. The concept behind each method is described in Figure 1, and we developed these methods in order to overcome traditional challenges associated with the vesicle fusion method while also enhancing user-friendly characteristics to expand the use of SLB platforms across the wider scientific community. For example, the SALB technique entails simple sample preparation, works with many types of surfaces, and is compatible with biologically important lipid compositions. Likewise, the bicelle method also has simple sample preparation under fully aqueous conditions, is robust production-wise, and requires significantly smaller amounts of lipid consumption. Herein, we introduce our ongoing development of both methods, highlighting key parameters and discussing important application examples from our group and the field. While the vesicle fusion technique has many advantages, we hope that this Feature Article will encourage

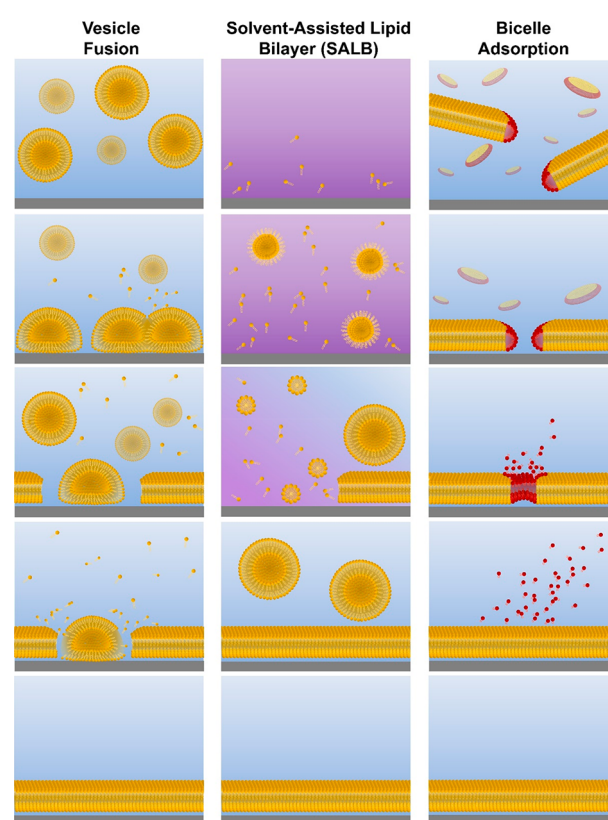


Figure 1. Schematic comparison of the vesicle fusion, SALB, and bicelle methods to form supported lipid bilayers. (Left column) The vesicle fusion method involves vesicle adsorption, deformation, and eventual rupture on a solid surface. The SLB formation process critically depends on vesicle–substrate interactions, which must be sufficiently strong to induce rupture via vesicle–substrate and/or vesicle–vesicle interactions. Typically, this method works only on a narrow range of material surfaces, particularly silica-based ones. (Middle column) The SALB method is based on depositing long-chain phospholipids in a water-miscible organic solvent, followed by a solvent-exchange step with aqueous solution. Initially, the phospholipid molecules in organic solvent self-assemble into inverted micelles and/or remain in the monomeric state and attach to the surface in an equilibrium with bulk lipids. During the solvent-exchange step, the bulk liquid transitions from predominately organic solvent to fully aqueous solution. Consequently, phospholipid molecules within the system begin to form lamellar-phase structures, leading to SLB formation on the surface. (Right column) Bicelles contain long-chain (yellow) and short-chain (red) phospholipids and are disklike nanostructured assemblies in aqueous solution. If there is an attractive bicelle–surface interaction, then bicelles adsorb onto the surface and then can fuse with one another. Provided the total lipid concentration is sufficiently low, long-chain phospholipid molecules remain attached on the surface and form an SLB while short-chain phospholipid molecules leave the surface as monomers. The outcome is a complete SLB consisting of long-chain phospholipids, and the entire fabrication process occurs under aqueous conditions.

scientific researchers to look beyond the vesicle fusion alone and view the SALB and bicelle methods as emerging options that complement, and in some cases go beyond, the vesicle fusion method and broaden application possibilities.

■ SALB METHOD

We begin by introducing the SALB method. Depending on the solvent environment, it is well known that phospholipids can self-assemble into a variety of structures such as inverted

micelles, normal micelles, and vesicles or remain as monomers. Thus, it is possible to control the adsorption and self-assembly of phospholipid molecules on a solid support by varying the bulk solvent.⁶⁷ Early work in the field demonstrated that phospholipid molecules in a water-miscible organic solvent (isopropanol) can be deposited on a silicon dioxide surface, and then the solvent was exchanged from isopropanol to aqueous solution.⁶⁸ The solvent-exchange process occurred gradually as water–isopropanol mixtures with increasing water fractions were introduced step by step. As the solution environment changed from isopropanol to aqueous solution, the phospholipids in the system underwent a series of phase transitions, shifting from inverted micelles and monomers to forming micelles and eventually lamellar-phase vesicles. Accordingly, an SLB formed on the silicon dioxide surface once the solution environment became predominately aqueous, and additional solvent exchange ensured that the resulting SLB was formed in an aqueous environment.

On the basis of the solvent-exchange concept, we developed the versatile SALB method which can rapidly form SLBs on a wide range of surfaces.⁶⁹ In the SALB protocol, lipid molecules are deposited in a water-miscible organic solvent, and then a single solvent-exchange step is performed with aqueous buffer so that an SLB can be quickly formed. Importantly, we identified that the SALB method works on both silicon dioxide and gold surfaces. While vesicle fusion with zwitterionic lipid compositions works well on silicon dioxide surfaces, it does not usually work on gold surfaces; therefore, the successful fabrication of an SLB on a gold surface was an important demonstration of an advantageous feature of the SALB method (Figure 2). The SALB method also works to form lipid monolayers on hydrophobic surfaces such as alkanethiol-terminated gold. Furthermore, sample preparation with the SALB method only entails solubilizing lipid in an appropriate organic solvent. We also clarified the scope of possible water-miscible organic solvents; isopropanol had the best performance in terms of SLB quality, ethanol and methanol were moderately successful, and *n*-propanol was less effective.

We have also investigated the effects of lipid concentration on SLB formation quality, in turn yielding important practical and mechanistic insights.⁷⁰ In terms of performance, there is an optimal lipid concentration range (~ 0.1 to 0.5 mg/mL phospholipid in our experience) for forming high-quality, complete SLBs. At lower concentrations, SLB formation is incomplete due to insufficient lipid supply. At higher concentrations, there is a nucleation of additional lipid structures on top of the SLB, and the specific type of structure depends on the organic solvent. In isopropanol and *n*-propanol, elongated tubule-like structures protruded from the SLB while vesicle-like structures formed in ethanol. Mechanistically, these trends are related to the reversible equilibrium that exists between surface-adsorbed and bulk-phase phospholipid molecules in the organic solvent during the initial incubation step. At higher lipid concentrations, there is more adsorbed lipid, which translates into more nucleation sites from which SLB formation occurs.

These findings led us to develop an initial video guide to the SALB method⁷¹ as well as to develop a comprehensive, refined protocol⁷² that covers the full scope of experimental steps, design strategies, applications, and troubleshooting needs. In the course of protocol development, we identified several key factors that affect SALB fabrication outcomes and also demonstrate how the application of the SALB method is

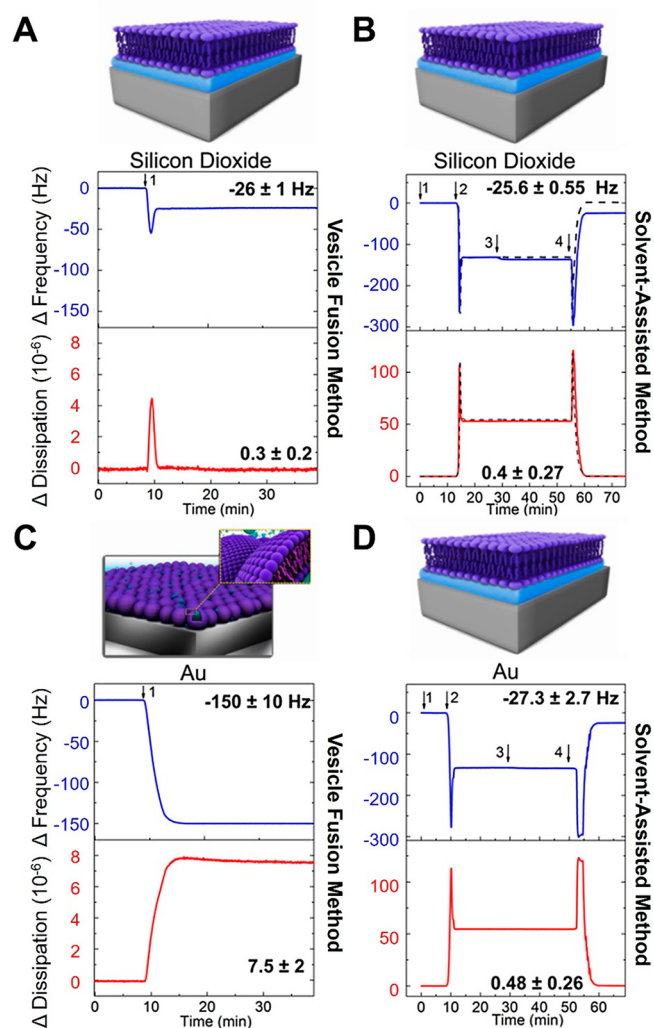


Figure 2. Comparison of the vesicle fusion and SALB methods on silicon dioxide and gold surfaces. Quartz crystal microbalance-dissipation (QCM-D) experiments were conducted to characterize the SLB formation process. Real-time QCM-D frequency shifts (blue) and energy dissipation shifts (red) were recorded for each experiment. Panels (A and C) show vesicle fusion data on silicon dioxide and gold surfaces, respectively. The baseline signal was recorded in aqueous buffer solution (10 mM Tris [pH 7.5] with 150 mM NaCl), and then 1,2-dioleoyl-*sn*-glycero-3-phosphocholine (DOPC) lipid vesicles in equivalent buffer solution were added at arrow 1. Panels (B and D) show corresponding data for DOPC SLB formation using the SALB method. Arrows 1–4 correspond to the baseline signal in aqueous buffer solution, solvent exchange to isopropanol, the addition of 0.5 mg/mL DOPC lipid in isopropanol, and solvent exchange back to aqueous buffer solution, respectively. The final QCM-D frequency shifts (blue) and energy dissipation shifts (red) are presented above each graph per experimental series. The data indicate that vesicle fusion forms SLBs on silicon dioxide surfaces but is not able to form SLBs on gold surfaces. By contrast, the SALB method is able to form SLBs on silicon dioxide and gold surfaces. Adapted with permission from ref 69. Copyright 2014 American Chemical Society.

providing new insights into lipid–substrate interactions. We discuss pertinent factors below.

Flow Dynamics. A key factor in the SALB procedure is the rate of solvent exchange, and it must be empirically optimized for the flow geometry of a chosen microfluidic chamber and other conditions such as the bulk lipid concentration. In

general, if the flow rate is high, then the SALB procedure can result in incomplete bilayer formation because the amount of lipid supply in the bulk solution is too low.⁶⁹

To explain this trend, we have conducted time-lapse fluorescence microscopy experiments to measure the rate of SLB formation within a microfluidic chamber, and supporting numerical simulations showed that the formation rate is linked to the solvent displacement velocity⁷³ (Figure 3).

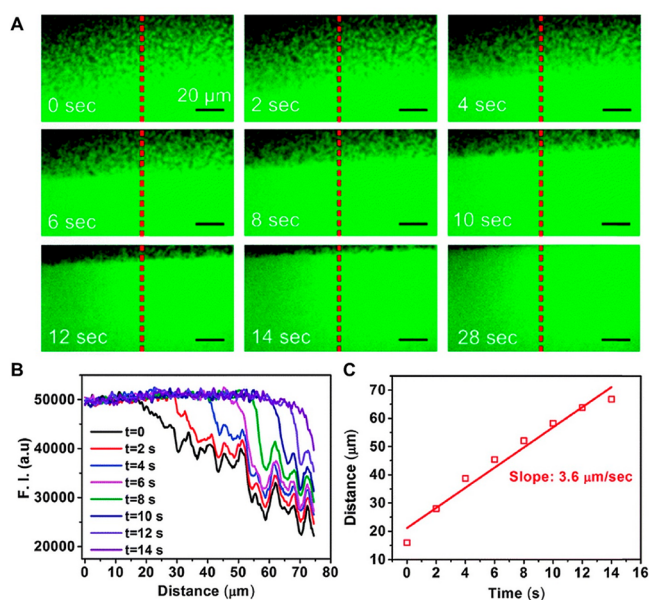


Figure 3. Observation of supported lipid bilayer formation on a glass surface within a microfluidic chamber. (A) Time-lapsed fluorescence micrographs of DOPC SLB formation by the SALB method. The lipid mixture was 99.9 mol % DOPC and 0.1 mol % 1,2-dioleoyl-*sn*-glycero-3-phosphoethanolamine-*N*-(lissamine rhodamine B sulfonyl) (ammonium salt) (Rh-PE), the total phospholipid concentration was 0.5 mg/mL in isopropanol, and the aqueous buffer solution for solvent exchange was 10 mM Tris [pH 7.5] with 150 mM NaCl. The fluorescence signal originates from fluorescently labeled Rh-PE phospholipids within the lipid mixture. The time stamps are relative to the first micrograph, and the solvent flow is in the upward direction parallel to the dashed red line. The contrast between the fluorescence and no-fluorescence regions indicates the evolving SLB front. Scale bars: 20 μm . (B) Fluorescence intensity profile of the evolving SLB front in the dashed line direction at different time points based on the micrographs in panel (A). (C) Time-dependent SLB front position, which is defined as the position where the fluorescence intensity profiles in panel (B) begin to drop. Adapted with permission from the PCCP Owner Societies from ref 73. Copyright 2015 Royal Society of Chemistry.

Additionally, we have developed a phenomenological model to describe the SALB formation process, and it included a volume-averaged treatment of the solvent mixing process.⁷⁴ On the basis of analyzing experimental data with this model, it was determined that lipid monomers are the main adsorbing species involved in the SLB formation process.

Understanding how flow dynamics affect SLB formation success not only offers fundamental insights into the SALB method but also provides practical guidance for designing improved measurement systems. For example, we conducted theoretical simulations of the solvent flow in order to design a specialized microfluidic chamber for optimal bilayer formation

with the SALB method, and it is compatible with atomic force microscopy experiments.⁷⁵

Substrates. The SALB method is able to form SLBs on a wide range of substrates that are typically incompatible with the vesicle fusion method. An important distinction is that, for vesicle fusion, the vesicle–substrate interaction energy must be sufficiently high not only for lipid–substrate adhesion but also to induce the rupture of adsorbed vesicles, whereas the energy barrier for the SALB method is lower because it does not require the rupture of adsorbed vesicles. In our experience, SLB formation is possible with the SALB method as long as there is an attractive lipid–substrate interaction (which is also controllable on a given surface by a factor such as the solution pH; e.g., ref 72), and key examples of suitable substrates include chrome, indium tin oxide, and titanium oxide.⁷⁰ We have also conducted more detailed studies on 1-palmitoyl-2-oleoyl-*sn*-glycero-3-phosphocholine (POPC) SLB formation on aluminum oxide surfaces with the QCM-D technique and extended-DLVO modeling and identified that zwitterionic SLBs appear to have larger bilayer–substrate separation distances than equivalent SLBs on silicon dioxide surfaces.^{76,77} This difference occurs because aluminum oxide surfaces have a thicker layer of coupled interfacial water molecules, which also causes greater hydrodynamic coupling and reduced lateral lipid diffusion in SLBs on aluminum oxide.⁷⁸ In the future, it would be advantageous to extend this line of investigation using powerful surface-sensitive techniques such as neutron reflectometry as well. It has also been possible to fabricate anionic SLBs on aluminum oxide surfaces using the SALB method and lipids with anionic headgroups preferred to reside in the lower bilayer leaflet due to attractive electrostatic interactions with the positively charged aluminum oxide surface.⁷⁹

In addition to oxide surfaces, the SALB method has also proven successful at forming SLBs on chemical vapor deposited (CVD) graphene surfaces.⁸⁰ The as-fabricated CVD graphene surface was hydrophobic so a lipid monolayer formed on pristine surfaces, while an SLB was successfully formed on oxygen-plasma-treated CVD graphene because the oxygen plasma treatment rendered the surface hydrophilic. By contrast, it was not possible to form SLBs on CVD graphene by using vesicle fusion. In addition, the SALB method has proven useful in forming SLBs on industrially useful surfaces such as conducting polymers⁸¹ as well as on nanoporous gold surfaces.⁸²

Cholesterol Incorporation. There has long been interest in developing cholesterol-enriched SLBs as cholesterol is a biologically important molecule that plays a key role in modulating membrane properties such as fluidity and rigidity.^{83,84} The cholesterol fraction in cellular membranes can exceed 60 mol % depending on the cell type and biological status; however, it is difficult to form SLBs with cholesterol fractions exceeding 20 mol % when using the vesicle fusion method. Above this fraction, cholesterol-enriched vesicles are typically too stiff to rupture in the adsorbed state, while there have been some recent efforts to fabricate SLBs from vesicles containing higher cholesterol fractions in aqueous solutions containing divalent cations.^{53,54}

Toward establishing a robust fabrication approach, the SALB method has been proven to be adept because it bypasses the need to induce vesicle rupture and instead supports bottom-up SLB assembly from phospholipid and cholesterol molecules. Indeed, the SALB method is able to form cholesterol-rich DOPC SLBs with high cholesterol fractions, as we have

demonstrated under aqueous buffer conditions consisting of 10 mM Tris [pH 7.5] with 150 mM NaCl. In particular, using the SALB method, we have identified optimal conditions for fabricating cholesterol-rich DOPC SLBs with well-controlled cholesterol fractions ranging between 0 and ~60 mol %.⁸⁵ The cholesterol-containing SLBs produced by the SALB method typically had two phases composed of a fluidic phospholipid-rich phase and cholesterol-rich domains, the latter of which grew larger at higher cholesterol fractions, especially at 20 mol % and higher cholesterol fractions in the precursor mixture (equating to around 30 mol % cholesterol in the SLB, as determined by methyl- β -cyclodextrin extraction QCM-D experiments^{86,87}). In these experiments, a DOPC-cholesterol SLB was initially formed, and then methyl- β -cyclodextrin was injected into the measurement chamber to extract cholesterol from the SLB.⁸⁵ The QCM-D frequency shift associated with cholesterol removal was measured, and the molar fraction of cholesterol within the SLB could be determined by applying the Sauerbrey equation, which relates QCM-D frequency shifts to changes in adsorbed mass for *rigid* SLB platforms.⁸⁵ Depending on the available techniques and study objective, it is also possible to employ other experimental strategies to quantify the cholesterol fraction within an SLB, such as using deuterated and hydrogenated cholesterol molecules in conjunction with neutron reflectometry measurements.⁵⁴

In our experimental studies, we have also attempted the formation of cholesterol-rich DOPC SLBs using extruded DOPC-cholesterol vesicles under equivalent aqueous buffer conditions (10 mM Tris [pH 7.5] with 150 mM NaCl). In this case, SLB formation was limited to lipid compositions with up to 20 mol % cholesterol. Comparatively, methyl- β -cyclodextrin extraction QCM-D experiments showed that cholesterol-containing SLBs formed by the vesicle fusion method typically had a *lower* molar fraction of cholesterol in the SLB than what was used in the vesicle precursor mixture (~20 mol % cholesterol in DOPC-cholesterol lipid vesicles versus ~10 mol % cholesterol in the DOPC-cholesterol SLB), while there was closer agreement between the molar fraction of cholesterol in the SLB formed using the SALB method and the molar fraction of cholesterol in the isopropanol mixture (the amount of cholesterol in the SLB was slightly *higher* than that in the input mixture).⁸⁵ In addition, we have observed that membrane fluidity decreased at higher cholesterol fractions within the fluid-phase regions of DOPC-cholesterol SLBs formed by the SALB method in accordance with expected trends, as determined by fluorescence recovery after photobleaching (FRAP) measurements.⁸⁵ Of note, the level of membrane fluidity (indicated by the diffusion coefficient of lateral lipid motion) within cholesterol-containing DOPC SLBs returned to the level found within cholesterol-free DOPC SLBs upon treatment with methyl- β -cyclodextrin to extract the cholesterol molecules.⁸⁵

A follow-up study investigating the SALB formation of cholesterol-rich DOPC SLBs demonstrated that SLBs with less than 20 mol % cholesterol possibly have coexisting liquid-disordered and liquid-ordered phases, while SLBs with higher cholesterol fractions are primarily in the liquid-ordered phase due to the cholesterol condensing effect.⁸⁸ Additionally, it has been possible to fabricate cholesterol-rich DOPC SLBs with ~63 mol % cholesterol, which approaches its solubility limit and led to the first example of observing phase coexistence in the β region of cholesterol–phospholipid mixtures on an SLB platform⁸⁹ (Figure 4). The two phases have a striped

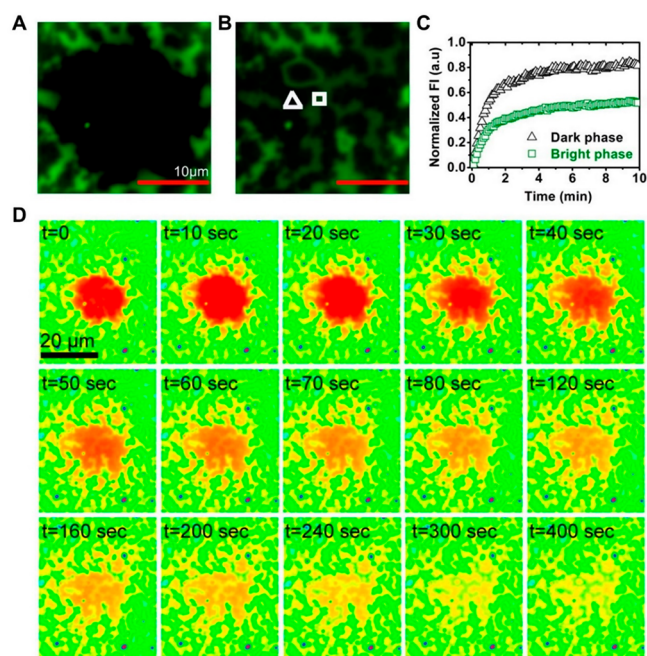


Figure 4. Fluorescence recovery after photobleaching (FRAP) analysis of lateral lipid diffusion in a cholesterol-rich SLB exhibiting stripe topography. The cholesterol-rich SLB was formed on a glass surface by using a lipid mixture composed of 40 mol % DOPC, 60 mol % cholesterol, and 0.5 wt % Rh-PE lipid. The total lipid concentration was 0.5 mg/mL in isopropanol, and the aqueous buffer solution for solvent exchange was 10 mM Tris [pH 7.5] with 150 mM NaCl. The molar fraction of cholesterol in the SLB was determined to be ~63 mol % via a methyl- β -cyclodextrin extraction QCM-D assay and showed evidence of two coexisting phases by fluorescence microscopy. (A and B) Close-up micrographs of a bleached spot in the SLB (A) immediately and (B) 10 min after photobleaching. (C) Time-lapse fluorescence intensity recovery curves for the bright- and dark-phase regions of the SLB. The specific intensity profiles correspond to the triangle and square marker positions in panel (B). (D) Time-lapse sequence of FRAP micrographs depicting fluorescence recovery in each phase (bright- and dark-phase regions are indicated by yellow and green, respectively, while red depicts the bleached spot within the SLB). Adapted with permission from ref 89. Copyright 2014 American Chemical Society.

morphology, and lateral lipid diffusion within each phase was generally favored over crossing across phase boundaries. Thus, the SALB method has provided a useful approach to fabricating cholesterol-rich DOPC SLBs that can exhibit phase coexistence in the β region of cholesterol–phospholipid mixtures and has further demonstrated a broadly useful approach to fabricating SLBs with tunable cholesterol fractions.

Lipid Composition. Aside from incorporating sterols, it is also possible to form SLBs containing numerous types of phospholipids that have proven difficult to work with when using conventional fabrication methods. For example, it is possible to form gel-phase SLBs with ~20% greater adlayer density compared to that of fluid-phase SLBs on account of tighter molecular packing.⁷⁰ In another recent project, we investigated the nanomechanical properties of SLBs formed from mixtures of fluid-phase and gel-phase phospholipids and were able to modulate the magnitudes of lateral lipid diffusion and bilayer rigidity on the basis of controlling the molar ratio of the two phospholipid components.⁹⁰ The ability to fabricate gel-phase SLBs has also proven useful in studying the intermolecular rotation of molecular machines.⁹¹

For biological applications, the SALB method has also proven advantageous because it can be difficult to form biologically relevant SLBs due to high anionic lipid fractions and/or lipid curvature effects that might impede vesicle fusion or require specialized experimental conditions. We have shown that the SALB method is able to form bacterial-cell-membrane-mimicking SLBs composed of phosphatidylethanolamine and phosphatidylglycerol lipids⁹² as well as SLBs containing significant amounts of highly anionic phosphatidylinositol lipids.⁹³

BICELLE METHOD

While the SALB method has many advantages, it does require initial deposition in an organic solvent and thus calls for extensive washing postfabrication to minimize the potential for organic solvent residues in the SLB^{68,69} as well as potentially poses some limitations for incorporating certain SLB components such as membrane proteins due to possible denaturation in organic solvent–water mixtures during the solvent-exchange process.⁹⁴ Considering these factors, we have also investigated the development of streamlined SLB fabrication methods that are fully conducted under aqueous solution conditions. Toward this goal, we became interested in bicelles which are widely used in structural biology as a suitable membranous environment for hosting membrane proteins.^{95–97} Consequently, a wide range of solution-phase studies have been published over the years describing how bicelle structure and properties are influenced by factors such as the phospholipid composition, total lipid concentration, ratio of long-chain phospholipids to short-chain phospholipids (denoted as the q ratio), and other solution and processing conditions.^{98–100}

One of the most attractive features of bicelles is that they are easy to prepare and do not require specialized equipment or skills (Figure 5). Briefly, a dry, thin film of phospholipids is hydrated in aqueous buffer solution, followed by vortex mixing, and the lipid suspension is then subjected to a series of freeze–thaw–vortex cycles. In each cycle, the bicellar suspension is quickly frozen in liquid nitrogen for ~ 1 min, heated in a moderately warm (ca. 60–70 °C) water bath for ~ 5 min, and then moderately vortex mixed. Around 5–10 cycles are completed per sample, and only standard laboratory equipment is needed.

The ease of sample preparation makes bicelles an attractive tool for fabricating SLBs on solid supports. Early efforts focused on zwitterionic lipid compositions and demonstrated that bicelle deposition can lead to SLB formation on silicon chips.¹⁰¹ It was also possible to form SLBs on silicon dioxide surfaces, although it was noted that bicelles, in the case of some lipid compositions, needed to be doped with a cationic surfactant in order to inhibit the formation of adsorbed bicelle multilayers.¹⁰² Additional work revealed that careful optimization of bicelle parameters, especially the q ratio, is important because the inclusion of relatively high concentrations of short-chain phospholipids can cause the formation of low-quality SLBs due to membrane-disruptive effects.¹⁰³

One aspect that stood out from these early works is that the total lipid concentrations were rather high and typically in the range of 0.25 and 0.8 mg/mL long-chain phospholipid. These lipid concentrations are comparable to or even higher than those used with vesicle fusion, and this issue deserved further attention from the practical perspective of minimizing lipid cost and consumption as well as from the fundamental perspective

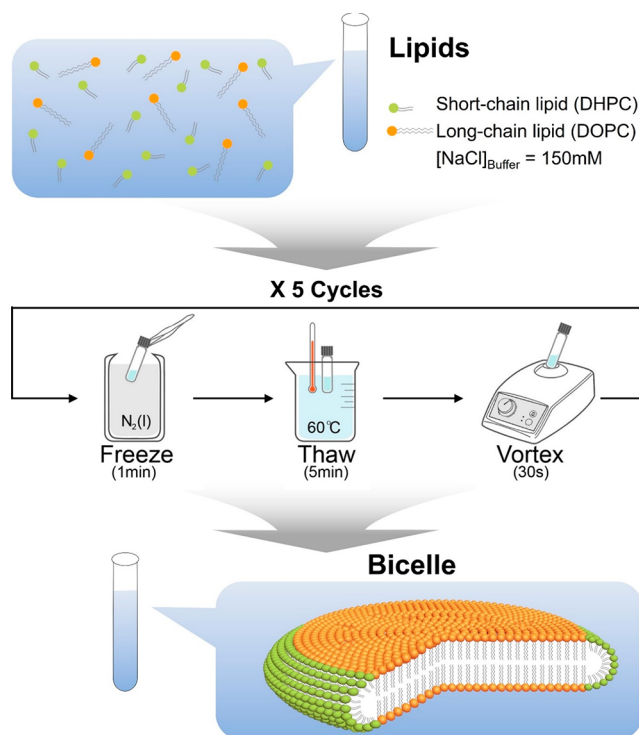


Figure 5. Overview of bicelle sample preparation. A combination of short-chain and long-chain phospholipids is hydrated in aqueous buffer solution and then undergoes a series of freeze–thaw–vortex cycles before dilution to the experimental concentration. We typically use at least five cycles as part of our sample preparation process. Adapted with permission from ref 101. Copyright 2019 American Chemical Society.

of understanding mechanistic aspects behind the SLB formation process when using bicelles.

Consequently, we first investigated how the total lipid concentration and q ratio of bicelles can be modulated in order to optimize SLB formation on silicon dioxide surfaces.¹⁰⁴ We conducted QCM-D and time-lapse fluorescence microscopy imaging experiments to evaluate bicelle adsorption, deformation, and fusion along with SLB formation on silicon dioxide surfaces and identified a three-step mechanism. First, bicelles adsorb onto and become deformed on the silicon dioxide surface. Second, adsorbed bicelles fuse together along the edges. Third, long-chain phospholipids self-assemble to form a complete SLB while short-chain phospholipids do not reside within the SLB and instead return to the bulk solution. Depending on the total lipid concentration and q ratio, the short-chain phospholipids in the bulk solution are present as either monomers or micelles, and fine-tuning the system to favor the monomeric state is important because only short-chain phospholipid micelles disturb the SLB whereas monomers do not.

Importantly, we discovered that high-quality SLBs are formed when the total lipid concentration was relatively low, equating to around 0.024 mg/mL long-chain phospholipid and below. This concentration is more than 10 times lower than in previous bicelle studies and is also significantly lower than typical lipid concentrations used in vesicle fusion and SALB experiments. In this low concentration range, there are a sufficient number of short-chain phospholipid molecules within bicelles to support bicelle adsorption, deformation, and fusion (via membrane softening), while after SLB formation occurs the

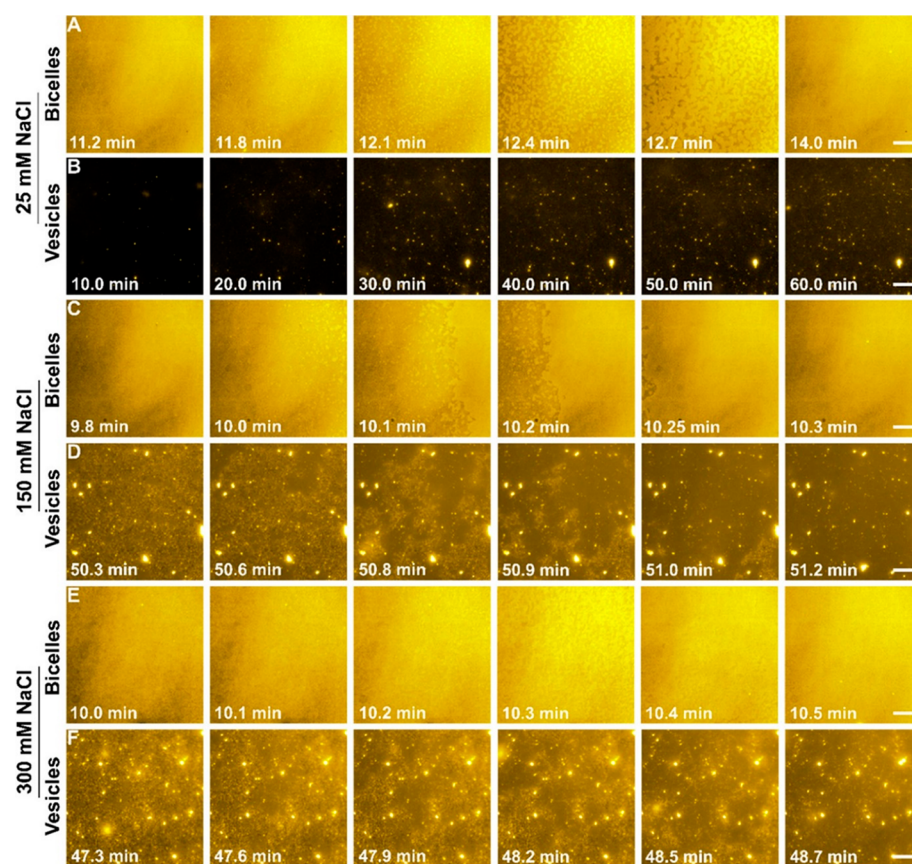


Figure 6. Time-lapse fluorescence microscopy imaging of bicelle and vesicle adsorption onto glass surfaces in aqueous buffer containing different NaCl concentrations. The long-chain phospholipid composition was 99.5 mol % DOPC and 0.5 mol % Rh-PE, the short-chain phospholipid was 1,2-dihexanoyl-*sn*-glycero-3-phosphocholine (DHPC), the q ratio was 0.25, the long-chain phospholipid concentration was 0.031 mM, and the aqueous buffer solution was 10 mM Tris [pH 7.5] with varying NaCl salt concentrations as specified. The micrographs show (A) the DOPC/DHPC lipid bicelle and (B) DOPC lipid vesicle addition in 25 mM NaCl salt, (C) bicelle and (D) vesicle addition in 150 mM NaCl salt, and (E) bicelle and (F) vesicle addition in 300 mM NaCl salt. Bicelles or vesicles were added starting from $t = 0$ min. Scale bars: 20 μm . Note that the DOPC lipid vesicles were prepared by the same freeze–thaw–vortex cycling method as for the DOPC/DHPC lipid bicelles for direct comparison; the vesicles were not extruded or sonicated in this case. Reproduced with permission from ref 101. Copyright 2019 American Chemical Society.

short-chain phospholipids are present in the monomeric state within the bulk solution. Thus, the SLB quality is high and not compromised by short-chain phospholipid micelles. Operationally, this finding was interesting because the vesicle fusion and SALB methods are typically more effective at relatively *higher* lipid concentrations while the bicelle method is more effective at *lower* lipid concentrations. The experimental results also provided mechanistic insight into the differences between vesicle fusion, in which case adsorbed vesicles undergo strong surface-induced deformation that triggers fusion, rupture, and reassembly of long-chain phospholipids on the material surface, and bicelle-mediated SLB formation, in which case adsorbed bicelles naturally exhibit high deformation due to the disklike architecture of bicelles. Therefore, bicelle fusion plays a more prominent role in driving the SLB formation process along with considering the short residence time of short-chain phospholipids in the planar configuration of an evolving SLB.

In a follow-up study, we also compared the effect of bulk NaCl concentration on bicelle and vesicle adsorption onto silicon dioxide surfaces.¹⁰⁵ The bicelles contained a mixture of long-chain and short-chain phospholipids whereas the vesicles contained only long-chain phospholipids. Both samples were prepared using an identical freeze–thaw–vortex protocol that is commonly used to make bicelles (cf. Figure 5). While it is generally preferable to subsequently extrude or sonicate vesicles

to optimize their size distribution for efficient SLB formation, an additional step of this kind was not done for the DOPC lipid vesicles in our case because the objective was to directly compare the effects of DOPC/DHPC and DOPC lipid compositions using the bicelle preparation protocol.

The vesicle and bicelle samples were initially prepared in 150 mM NaCl and diluted in the appropriate NaCl solution. As a result, the vesicle samples in <150 mM NaCl and >150 mM NaCl solutions had negative and positive osmotic pressures, respectively, whereas osmotic pressure effects are negligible in bicelle samples due to the compact disklike architecture of bicelles. In addition, the lipid–substrate interaction strength for both bicelles and vesicles varied according to the NaCl solution, with more attractive interactions at higher salt concentrations due to charge shielding. At 50 mM and higher NaCl concentrations, it was possible to fabricate SLBs using bicelles, and the formation kinetics were similar in all cases. It was also possible to fabricate SLBs using bicelles at lower NaCl concentrations, albeit with moderately slower formation kinetics. By contrast, vesicles ruptured on silicon dioxide surfaces at 50 mM and higher NaCl concentrations although the SLB quality was highly variable, including the presence of unruptured vesicles on the surface. At lower NaCl concentrations, vesicle adsorption was modest to negligible and SLB formation did not occur. Corresponding fluorescence micro-

graphs for the bicelle and vesicle cases under different NaCl conditions are presented in Figure 6. Together, the findings demonstrated that bicelles are versatile tools for fabricating SLBs on silicon dioxide surfaces under varying environmental conditions. On the basis of these mechanistic insights, we have also further investigated SLB formation using bicelles on different surfaces and with different lipid compositions as discussed below.

Bicelle–Substrate Interactions. Another key area of focus has been exploring how lipid bicelles adsorb onto different solid supports and the role of membrane–surface interactions. We approached this topic by testing the adsorption of lipid bicelles with a wide range of membrane surface changes (achieved by using 1,2-dioleoyl-*sn*-glycero-3-phospholipids with different headgroups) onto silicon dioxide, titanium oxide, and aluminum oxide surfaces.¹⁰⁶ On negatively charged silicon dioxide surfaces, highly positively charged bicelles demonstrated strongly attractive electrostatic interactions with the solid support, as indicated by one-step SLB formation kinetics. Moderately positively charged bicelles and zwitterionic bicelles also formed SLBs on silicon dioxide surfaces and had two-step formation kinetics. On the other hand, negatively charged bicelles did not form SLBs due to electrostatic repulsion and either adsorbed to form an intact bicelle layer or did not adsorb if the charge repulsion was too significant. Interestingly, distinct trends were observed on negatively charged titanium oxide and positively charged aluminum oxide surfaces, and these trends could be rationalized by taking into account that the two surfaces, but not silicon dioxide surfaces, have strong hydration repulsion forces as well.^{76,107,108} On titanium oxide, only positively charged bicelles formed SLBs and had thick hydration layers separating the SLB from the underlying surface. On aluminum oxide, negatively charged bicelles formed SLBs whereas positively charged and zwitterionic bicelles adsorbed but did not rupture. From a broader perspective, these findings further demonstrate that vesicles and bicelles have distinct adsorption behaviors on various surfaces and can guide the selective formation of SLBs and adsorbed bicelle layers on different target surfaces. Indeed, for depositing membrane proteins on solid supports, the disklike architecture of an adsorbed, intact bicelle may be advantageous in order to provide a large membranous environment.

Cholesterol Incorporation. As discussed above, it is often difficult to fabricate SLBs from vesicles containing more than 20 mol % cholesterol. While testing bicelles, we have observed that DOPC/DHPC lipid bicelles with as much as 60 mol % cholesterol input can adsorb and rupture on silicon dioxide surfaces, highlighting the role that short-chain phospholipids play in softening the bicellar membrane and enhancing the rupture potential.¹⁰⁹ Bicelles with up to 30 mol % cholesterol formed complete SLBs as determined by QCM-D measurements, while bicelles with larger cholesterol fractions ruptured but did not form complete SLBs due to the presence of some unruptured bicelles. Among complete SLBs, methyl- β -cyclodextrin extraction QCM-D experiments revealed that the bicelle and SALB methods achieved similar performance levels in terms of the molar fraction of cholesterol that can be incorporated within an SLB, reaching around at least 40 mol % cholesterol in the bicelle case. Another notable point is that the bicelle method yielded homogeneous SLBs at high cholesterol fractions, whereas the SALB method results in visible phase separation characterized by a cholesterol-depleted,

phospholipid-rich fluid phase and a cholesterol-enriched dense phase (Figure 7).

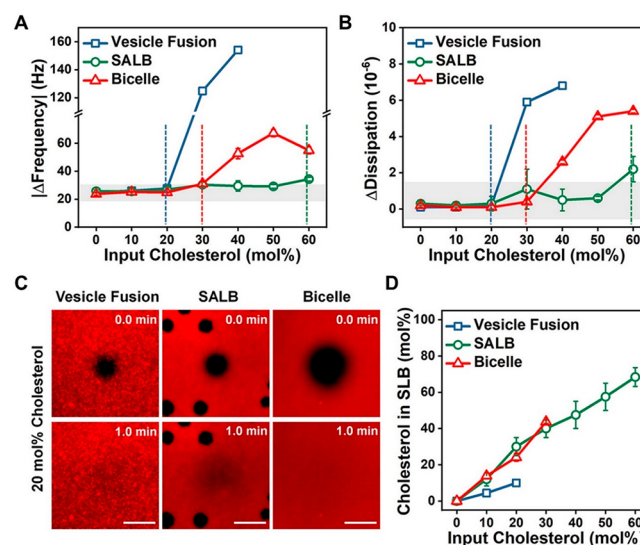


Figure 7. Comparison of cholesterol-rich SLB fabrication on silicon dioxide surfaces by vesicle fusion, SALB, and bicelle methods. For bicelles, the long-chain phospholipid was DOPC, the short-chain phospholipid was DHPC, the q ratio was 0.25, the long-chain phospholipid concentration was 0.031 mM, and the aqueous buffer solution was 10 mM Tris [pH 7.5] with 150 mM NaCl. For the SALB method, the DOPC lipid concentration was 0.3 mg/mL in isopropanol and the aqueous buffer solution for solvent exchange was 10 mM Tris [pH 7.5] with 150 mM NaCl. For vesicle fusion, DOPC lipid vesicles were extruded through track-etched polycarbonate membranes with 50-nm-diameter pores, the total lipid concentration was 0.15 mg/mL, and the aqueous buffer solution was 10 mM Tris [pH 7.5] with 150 mM NaCl. The final QCM-D measurement shifts are presented for the (A) frequency and (B) energy dissipation signals for SLB formation on silicon dioxide surfaces as a function of cholesterol fraction. Data correspond to the vesicle fusion (squares), SALB (circles), and bicelle (triangles) methods. The vesicle fusion method worked only at 20 mol % or smaller cholesterol fractions. (C) FRAP micrograph snapshots for 20 mol % cholesterol SLBs formed by the vesicle fusion, SALB, and bicelle methods. The long-chain phospholipid composition was 99.5 mol % DOPC and 0.5 mol % Rh-PE lipid in these experiments. Top and bottom micrographs depict SLBs immediately after photobleaching and after 1.0 min postbleaching, respectively. Scale bars: 20 μ m. (D) Molar fraction of cholesterol in SLB platforms as a function of the input cholesterol fraction used during the fabrication process (the molar fraction of cholesterol either in vesicles or bicelles or in the lipid mixture in organic solvent for the SALB method). The molar fraction of cholesterol within SLBs was determined by a methyl- β -cyclodextrin extraction QCM-D assay. Adapted with permission from ref 109. Copyright 2019 American Chemical Society.

Thus, the bicelle method has numerous advantages in terms of lipid consumption, robustness, and ease of sample preparation, which make it potentially ideal for expanding the use of conventional SLB platforms in laboratory settings and for manufacturing SLB platforms in industrial settings.

APPLICATION EXAMPLES

The SALB and bicelle methods have excellent potential to expand the use of SLB platforms because the methods are easy to implement and useful in a variety of application contexts. In this section, we introduce promising recent examples from our

group and others that demonstrate the utility of these fabrication techniques.

Drug Efficacy Monitoring. A recent collaboration with the Stanford University School of Medicine and University of California, San Francisco enabled us to evaluate the potency of a small-molecule inhibitor that inhibits the activity of the phosphatidylinositol (PI) 4-kinase III β (PI4K β) enzyme,¹¹⁰ which is necessary for converting PI to PI 4-phosphate (PI4P) as the first step in a two-step process that yields PI 4,5-bisphosphate [PI(4,5)P₂]. We developed a detergent-free QCM-D assay by using the SALB method to fabricate PI-enriched SLBs on a silicon dioxide surface⁹³ (Figure 8). We then added the PI4K β enzyme in order to catalyze the conversion of PI to PI4P, which could be detected and quantified by anti-PI4P antibody binding. To evaluate the inhibitory potency, we incubated different concentrations of the small-molecule inhibitor with the enzyme before adding the enzyme–small molecule mixture to the SLB platform. The inhibitory potency was determined on the basis of the concentration-dependent reduction in PIP4 production relative to the control experiment without inhibitor, and the computed 50% inhibitory value agreed with the biological assay results.

Extracellular Matrix Remodeling. SLB platforms functionalized with extracellular matrix (ECM) proteins provide an excellent model system for studying cell adhesion and related dynamic behaviors.^{111,112} In one interesting example, we investigated how adhered cells remodel the ECM protein-functionalized SLB surface by increasing the number of ECM proteins underneath the cell and depleting ECM proteins from the vicinity of the cell contact area.¹¹³ Lateral lipid diffusion of the SLB platform—an indicator of membrane fluidity—was necessary to support lateral reorganization of the ECM proteins, and the SALB method played a key role by enabling the fabrication of 0–40 mol % cholesterol-rich SLBs. With increasing cholesterol fraction, lateral lipid diffusion in the SLB decreased and accordingly the lateral reorganization of ECM proteins was reduced as well.

Surface-Enhanced Infrared Absorption Spectroscopy. The Lau group at the University of Massachusetts Amherst has recently employed the SALB method to produce SLBs on gold surfaces in order to study nanoparticle–membrane interactions using surface-enhanced infrared absorption spectroscopy (SEIRAS).¹¹⁴ The SEIRAS technique provides information about how nanoparticles interact with different components of the SLB platform, including hydrophobic and hydrophilic parts of the phospholipids along with interfacial water molecules on the SLB surface. Following this approach, it was determined that anionic carboxylic acid-functionalized polystyrene nanoparticles adsorb onto and penetrate into SLBs and cause changes in the interfacial water structure as well. By contrast, cationic amine-functionalized polystyrene nanoparticles remained on top of the SLB surface, as indicated by changes in the interfacial water structure only and negligible changes in the lipid signals.

Electrochemical Biosensing. The Daniel group at Cornell University has developed mammalian and bacterial-cell-membrane-mimicking SLB platforms on conducting polymer surfaces in order to study the membrane interactions of a bacterial toxin and an antibiotic.⁸¹ The SLBs could be formed using only the SALB method, while the vesicle fusion method was not successful, as verified by fluorescence microscopy and FRAP measurements. The SLB-coated conducting polymer surfaces could be integrated with electrochemical impedance

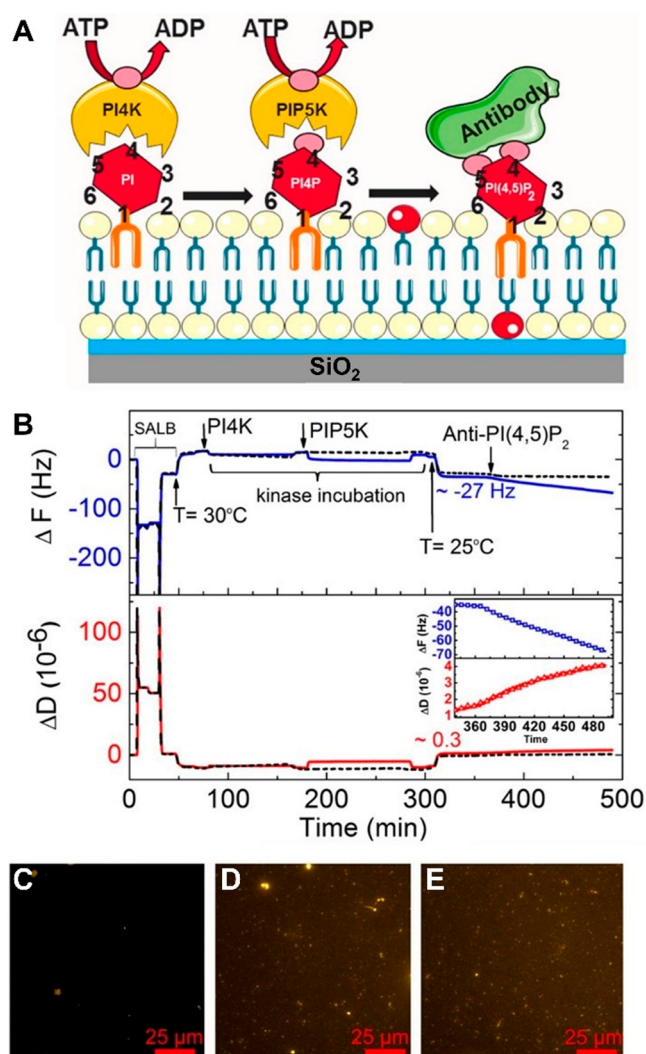


Figure 8. Development of a phosphatidylinositol-containing SLB platform for PI kinase inhibitor testing. (A) Scheme illustrating the two-step enzymatic conversion of PI lipid into PI(4,5)P₂ lipid. (B) QCM-D evaluation of PI(4,5)P₂ generation within a 10 mol % PI-containing SLB platform. Initially, the SLB was formed on a silicon dioxide surface using the SALB method, the lipid mixture was 90 mol % DOPC and 10 mol % PI, the total phospholipid concentration was 0.5 mg/mL in isopropanol, and the aqueous buffer solution for solvent-exchange was 10 mM Tris [pH 7.5] with 150 mM NaCl. PI4KIII β and PIP5K1A enzymes were then added sequentially to convert PI lipids to PI4P and then to PI₄,5P₂ lipids, respectively. PI₄,5P₂ lipid generation was then detected by the addition of anti-PI(4,5)P₂ antibody. The dashed line corresponds to the control experiment without the addition of PIP5K1A enzyme (hence, PI(4,5)P₂ lipid is not produced and no antibody signal is detected). Inset shows a magnified view of antibody binding step. Fluorescence micrographs for (C) 10 mol % PI-containing SLB and (D) 10 mol % PI(4,5)P₂-containing SLB, both after incubation with fluorescently labeled anti-PI(4,5)P₂ antibody. (E) Corresponding fluorescence micrograph for 10 mol % PI-containing SLB after enzymatic treatment with PI4K β and PIP5K α enzymes to yield PI(4,5)P₂ lipid, as indicated by fluorescently labeled antibody binding similar to the micrograph in panel (D). Adapted with permission from ref 93. Copyright 2016 American Chemical Society.

spectroscopy (EIS) in order to detect membrane interactions and distinguish between pore-forming and membrane-disruptive effects of the bacterial toxin and antibiotic, respectively. Importantly, by expanding the range of surfaces on which SLBs

can be formed, the SALB method opens the door to developing lipid-membrane-based bioelectronic devices, which can be utilized in multiplexed formats among various possibilities.

Taken together, these application examples being pursued by our group and other teams demonstrate how the SALB and bicelle methods can be useful in fabricating SLB coatings in a variety of contexts. Particular advantages come from fabricating SLB coatings on traditionally intractable surfaces in order to expand the range of compatible surface-sensitive measurement techniques.

■ CONCLUSIONS AND OUTLOOK

Our ongoing efforts to develop the SALB and bicelle methods have identified key opportunities where these methods can expand SLB fabrication options beyond what is possible with the vesicle fusion method alone. For example, the SALB method is compatible with many solid surfaces, which has led to numerous application examples already in use. At the same time, the development of the bicelle method is at an earlier stage than the SALB method; however, we already see strong merit in terms of sample preparation ease, low lipid consumption, and a robust fabrication process. These advantages of the bicelle method have led us to begin exploring larger-scale fabrication opportunities because it is a fully aqueous method and rather insensitive to deposition conditions such as the flow rate. In closing, we briefly summarize our views on the current progress and where we see upcoming research efforts headed for each method.

SALB Method. Over the past few years, we have extensively characterized the SALB process on different surfaces and understand how key parameters such as the lipid concentration and solvent-exchange rates affect performance outcomes. Currently, an ~ 0.1 mg/mL lipid concentration in organic solvent is necessary for forming complete SLBs, and it will be useful in developing microfluidic chips with suitable flow geometries to decrease the lipid consumption. Current lipid consumption is comparable to the vesicle fusion method; however, decreasing consumption would be advantageous. In addition, continued exploration of the SALB method by other research groups, both from within the membrane biophysics community and from other research areas, will help to develop the technology for different application areas while also refining the methodology. We see some of the largest opportunities in fabricating SLBs on metal surfaces such as gold in order to utilize other surface-sensitive measurement techniques.

Bicelle Method. In our experience, the bicelle method is a robust, fully aqueous way to routinely fabricate SLBs on silicon dioxide surfaces and works at 10-fold or lower lipid concentrations compared to the vesicle fusion and SALB methods. Depending on the material surface, our recent evidence demonstrates that bicelles will either fuse to form an SLB or remain intact in the adsorbed state. It will be important to continue studying the fundamental interactions between bicelles and material surfaces in order to build a strong mechanistic picture behind bicelle adsorption and learn how to control these formation pathways. Since bicelles can have disklike characteristics, it will also be advantageous not only to view bicelles as useful tools for forming SLBs but also to develop bicelle coatings depending on the application. For example, bicelles are excellent environments for reconstituting membrane proteins, and the development of bicelle coatings incorporating membrane proteins could lead to the development of highly functional bioanalytical platforms.

The SALB and bicelle methods are promising methods for forming SLB platforms and complement the fabrication capabilities of the vesicle fusion method. In developing these two new methods, our main objectives have been to simplify the sample preparation process, to increase the robustness of the SLB formation process, to expand the range of permissible lipid compositions, and to increase the scope of material surfaces on which SLBs can be formed. We hope that ongoing work by our group and others will continue the progress in this direction and increase the use of SLB platforms for fundamental and applied research across various scientific areas as well as spur the development of innovative technology platforms for applications such as biosensor coatings and medical diagnostics.

■ AUTHOR INFORMATION

Corresponding Author

Nam-Joon Cho – School of Materials Science and Engineering, Nanyang Technological University, Singapore 639798 Singapore; orcid.org/0000-0002-8692-8955; Email: njcho@ntu.edu.sg

Author

Joshua A. Jackman – School of Chemical Engineering, Sungkyunkwan University, Suwon 16419, Republic of Korea; orcid.org/0000-0002-1800-8102

Complete contact information is available at:
<https://pubs.acs.org/10.1021/acs.langmuir.9b03706>

Notes

The authors declare the following competing financial interest(s): The authors are inventors on patents and patent applications related to supported lipid bilayer coatings, including U.S. patent no. 10,427,124, PCT patent no. SG2018/050072, and PCT patent no. US2019/047518.

Biographies



Joshua A. Jackman is an Assistant Professor in the School of Chemical Engineering at Sungkyunkwan University. He received his B.S. degree in chemistry from the University of Florida and Ph.D. degree in materials science and engineering from Nanyang Technological University and was a postdoctoral scholar at the Stanford University School of Medicine. He has received fellowships from the Arnold and Mabel Beckman Foundation, National Science Foundation, and American Liver Foundation. His research interests lie at the interface of materials science and biotechnology towards developing biosensors, bioanalytical measurement platforms, and medical technologies.



Nam-Joon Cho is the MRS-Singapore Chair Professor in the School of Materials Science and Engineering and Principal Investigator of the Engineering in Translational Science group at Nanyang Technological University. He received his Ph.D. degree in chemical engineering from Stanford University and completed a postdoctoral fellowship at the Stanford University School of Medicine. His research focuses on engineering artificial lipid membrane and tissue platforms to probe biological systems and to develop enhanced therapeutic and drug delivery options that more effectively target infectious diseases, inflammatory disorders, and cancer, along with the development of pollen-based biomaterials. One of his most active research areas covers bioanalytical applications of label-free optical and acoustic sensors and surface functionalization with lipid bilayer coatings.

ACKNOWLEDGMENTS

This work was supported by the National Research Foundation of Singapore through a Proof-of-Concept grant (NRF2015NRF-POC0001-19).

REFERENCES

- Welsch, S.; Müller, B.; Kräusslich, H.-G. More than one door-budding of enveloped viruses through cellular membranes. *FEBS Lett.* **2007**, *581* (11), 2089–2097.
- Skotland, T.; Sandvig, K.; Llorente, A. Lipids in exosomes: current knowledge and the way forward. *Prog. Lipid Res.* **2017**, *66*, 30–41.
- Sezgin, E.; Levental, I.; Mayor, S.; Eggeling, C. The mystery of membrane organization: Composition, regulation and roles of lipid rafts. *Nat. Rev. Mol. Cell Biol.* **2017**, *18* (6), 361–374.
- Israelachvili, J. N.; Marčelja, S.; Horn, R. G. Physical principles of membrane organization. *Q. Rev. Biophys.* **1980**, *13* (2), 121–200.
- Wu, W.; Shi, X.; Xu, C. Regulation of T cell signalling by membrane lipids. *Nat. Rev. Immunol.* **2016**, *16* (11), 690.
- Ho, J. C.; Rangamani, P.; Liedberg, B.; Parikh, A. N. Mixing water, transducing energy, and shaping membranes: Autonomously self-regulating giant vesicles. *Langmuir* **2016**, *32* (9), 2151–2163.
- Edidin, M. Lipids on the frontier: a century of cell-membrane bilayers. *Nat. Rev. Mol. Cell Biol.* **2003**, *4* (5), 414.
- Lingwood, D.; Simons, K. Lipid rafts as a membrane-organizing principle. *Science* **2010**, *327* (5961), 46–50.
- Chan, Y.-H. M.; Boxer, S. G. Model membrane systems and their applications. *Curr. Opin. Chem. Biol.* **2007**, *11* (6), 581–587.
- Bally, M.; Bailey, K.; Sugihara, K.; Grieshaber, D.; Vörös, J.; Städler, B. Liposome and lipid bilayer arrays towards biosensing applications. *Small* **2010**, *6* (22), 2481–2497.
- Jackman, J. A.; Knoll, W.; Cho, N.-J. Biotechnology applications of tethered lipid bilayer membranes. *Materials* **2012**, *5* (12), 2637–2657.
- Mazur, F.; Bally, M.; Städler, B.; Chandrawati, R. Liposomes and lipid bilayers in biosensors. *Adv. Colloid Interface Sci.* **2017**, *249*, 88–99.
- Jackman, J. A.; Cho, N.-J. Model membrane platforms for biomedicine: case study on antiviral drug development. *Biointerphases* **2012**, *7* (1), 18.
- Tamm, L. K.; McConnell, H. M. Supported phospholipid bilayers. *Biophys. J.* **1985**, *47* (1), 105–113.
- Richter, R. P.; Bérat, R.; Brisson, A. R. Formation of solid-supported lipid bilayers: An integrated view. *Langmuir* **2006**, *22* (8), 3497–3505.
- Castellana, E. T.; Cremer, P. S. Solid supported lipid bilayers: From biophysical studies to sensor design. *Surf. Sci. Rep.* **2006**, *61* (10), 429–444.
- Czolkos, I.; Jesorka, A.; Orwar, O. Molecular phospholipid films on solid supports. *Soft Matter* **2011**, *7* (10), 4562–4576.
- Kiessling, V.; Domanska, M. K.; Murray, D.; Wan, C.; Tamm, L. K. Supported lipid bilayers. *Wiley Encyclopedia of Chemical Biology*; John Wiley & Sons: Hoboken, NJ, 2007; pp 1–12.
- Gözen, I.; Jesorka, A. Instrumental methods to characterize molecular phospholipid films on solid supports. *Anal. Chem.* **2012**, *84* (2), 822–838.
- Mingeot-Leclercq, M.-P.; Deleu, M.; Brasseur, R.; Dufrière, Y. F. Atomic force microscopy of supported lipid bilayers. *Nat. Protoc.* **2008**, *3* (10), 1654.
- Cho, N.-J.; Frank, C. W.; Kasemo, B.; Höök, F. Quartz crystal microbalance with dissipation monitoring of supported lipid bilayers on various substrates. *Nat. Protoc.* **2010**, *5* (6), 1096.
- Mashaghi, A.; Mashaghi, S.; Reviakine, I.; Heeren, R. M.; Sandoghdar, V.; Bonn, M. Label-free characterization of biomembranes: from structure to dynamics. *Chem. Soc. Rev.* **2014**, *43* (3), 887–900.
- Jackman, J. A.; Ferhan, A. R.; Cho, N.-J. Nanoplasmonic sensors for biointerfacial science. *Chem. Soc. Rev.* **2017**, *46* (12), 3615–3660.
- Hardy, G. J.; Nayak, R.; Zauscher, S. Model cell membranes: Techniques to form complex biomimetic supported lipid bilayers via vesicle fusion. *Curr. Opin. Colloid Interface Sci.* **2013**, *18* (5), 448–458.
- Keller, C.; Kasemo, B. Surface specific kinetics of lipid vesicle adsorption measured with a quartz crystal microbalance. *Biophys. J.* **1998**, *75* (3), 1397–1402.
- Keller, C.; Glasmästar, K.; Zhdanov, V.; Kasemo, B. Formation of supported membranes from vesicles. *Phys. Rev. Lett.* **2000**, *84* (23), 5443.
- Cremer, P. S.; Boxer, S. G. Formation and spreading of lipid bilayers on planar glass supports. *J. Phys. Chem. B* **1999**, *103* (13), 2554–2559.
- Reviakine, I.; Brisson, A. Formation of supported phospholipid bilayers from unilamellar vesicles investigated by atomic force microscopy. *Langmuir* **2000**, *16* (4), 1806–1815.
- Zhdanov, V. P.; Keller, C. A.; Glasmästar, K.; Kasemo, B. Simulation of adsorption kinetics of lipid vesicles. *J. Chem. Phys.* **2000**, *112* (2), 900–909.
- Klacar, S.; Dimitrievski, K.; Kasemo, B. Influence of surface pinning points on diffusion of adsorbed lipid vesicles. *J. Phys. Chem. B* **2009**, *113* (17), 5681–5685.
- Zhdanov, V. P.; Kasemo, B. Comments on rupture of adsorbed vesicles. *Langmuir* **2001**, *17* (12), 3518–3521.
- Cho, N.-J.; Wang, G.; Edvardsson, M.; Glenn, J. S.; Hook, F.; Frank, C. W. Alpha-helical peptide-induced vesicle rupture revealing new insight into the vesicle fusion process as monitored in situ by quartz crystal microbalance-dissipation and reflectometry. *Anal. Chem.* **2009**, *81* (12), 4752–4761.
- Cha, T.; Guo, A.; Zhu, X.-Y. Formation of supported phospholipid bilayers on molecular surfaces: Role of surface charge density and electrostatic interaction. *Biophys. J.* **2006**, *90* (4), 1270–1274.
- Biswas, K. H.; Jackman, J. A.; Park, J. H.; Groves, J. T.; Cho, N.-J. Interfacial forces dictate the pathway of phospholipid vesicle adsorption onto silicon dioxide surfaces. *Langmuir* **2018**, *34* (4), 1775–1782.

- (35) Jackman, J. A.; Špačková, B.; Linardy, E.; Kim, M. C.; Yoon, B. K.; Homola, J.; Cho, N.-J. Nanoplasmonic ruler to measure lipid vesicle deformation. *Chem. Commun.* **2016**, *52* (1), 76–79.
- (36) Oh, E.; Jackman, J. A.; Yorulmaz, S.; Zhdanov, V. P.; Lee, H.; Cho, N.-J. Contribution of temperature to deformation of adsorbed vesicles studied by nanoplasmonic biosensing. *Langmuir* **2015**, *31* (2), 771–781.
- (37) Jackman, J. A.; Kim, M. C.; Zhdanov, V. P.; Cho, N.-J. Relationship between vesicle size and steric hindrance influences vesicle rupture on solid supports. *Phys. Chem. Chem. Phys.* **2016**, *18* (4), 3065–3072.
- (38) Jackman, J. A.; Zhao, Z.; Zhdanov, V. P.; Frank, C. W.; Cho, N.-J. Vesicle adhesion and rupture on silicon oxide: Influence of freeze-thaw pretreatment. *Langmuir* **2014**, *30* (8), 2152–2160.
- (39) Jackman, J. A.; Choi, J.-H.; Zhdanov, V. P.; Cho, N.-J. Influence of osmotic pressure on adhesion of lipid vesicles to solid supports. *Langmuir* **2013**, *29* (36), 11375–11384.
- (40) Tero, R. Substrate effects on the formation process, structure and physicochemical properties of supported lipid bilayers. *Materials* **2012**, *5* (12), 2658–2680.
- (41) Sundh, M.; Svedhem, S.; Sutherland, D. S. Formation of supported lipid bilayers at surfaces with controlled curvatures: Influence of lipid charge. *J. Phys. Chem. B* **2011**, *115* (24), 7838–7848.
- (42) Pfeiffer, I.; Seantier, B.; Petronis, S.; Sutherland, D.; Kasemo, B.; Zäch, M. Influence of nanotopography on phospholipid bilayer formation on silicon dioxide. *J. Phys. Chem. B* **2008**, *112* (16), 5175–5181.
- (43) Boudard, S.; Seantier, B.; Breffa, C.; Decher, G.; Felix, O. Controlling the pathway of formation of supported lipid bilayers of DMPC by varying the sodium chloride concentration. *Thin Solid Films* **2006**, *495* (1–2), 246–251.
- (44) Dacic, M.; Jackman, J. A.; Yorulmaz, S.; Zhdanov, V. P.; Kasemo, B.; Cho, N.-J. Influence of divalent cations on deformation and rupture of adsorbed lipid vesicles. *Langmuir* **2016**, *32* (25), 6486–6495.
- (45) Reimhult, E.; Höök, F.; Kasemo, B. Temperature dependence of formation of a supported phospholipid bilayer from vesicles on SiO₂. *Phys. Rev. E: Stat. Phys., Plasmas, Fluids, Relat. Interdiscip. Top.* **2002**, *66* (5), 051905.
- (46) Cho, N.-J.; Jackman, J. A.; Liu, M.; Frank, C. W. pH-Driven assembly of various supported lipid platforms: A comparative study on silicon oxide and titanium oxide. *Langmuir* **2011**, *27* (7), 3739–3748.
- (47) Reimhult, E.; Höök, F.; Kasemo, B. Intact vesicle adsorption and supported biomembrane formation from vesicles in solution: Influence of surface chemistry, vesicle size, temperature, and osmotic pressure. *Langmuir* **2003**, *19* (5), 1681–1691.
- (48) Reviakine, I.; Rossetti, F. F.; Morozov, A. N.; Textor, M. Investigating the properties of supported vesicular layers on titanium dioxide by quartz crystal microbalance with dissipation measurements. *J. Chem. Phys.* **2005**, *122* (20), 204711.
- (49) Xu, S.; Szymanski, G.; Lipkowski, J. Self-assembly of phospholipid molecules at a Au (111) electrode surface. *J. Am. Chem. Soc.* **2004**, *126* (39), 12276–12277.
- (50) Lipkowski, J. Building biomimetic membrane at a gold electrode surface. *Phys. Chem. Phys.* **2010**, *12* (42), 13874–13887.
- (51) Pawlowski, J.; Juhaniewicz, J.; Güzelölu, A.; Şk, S. Mechanism of lipid vesicles spreading and bilayer formation on a Au(111) surface. *Langmuir* **2015**, *31* (40), 11012–11019.
- (52) Tero, R.; Ujihara, T.; Urisu, T. Lipid bilayer membrane with atomic step structure: supported bilayer on a step-and-terrace TiO₂(100) surface. *Langmuir* **2008**, *24* (20), 11567–11576.
- (53) Waldie, S.; Lind, T. K.; Browning, K.; Moulin, M.; Haertlein, M.; Forsyth, V. T.; Luchini, A.; Strohmeier, G. A.; Pichler, H.; Maric, S. Localization of cholesterol within supported lipid bilayers made of a natural extract of tailor-deuterated phosphatidylcholine. *Langmuir* **2018**, *34* (1), 472–479.
- (54) Waldie, S.; Moulin, M.; Porcar, L.; Pichler, H.; Strohmeier, G. A.; Skoda, M.; Forsyth, V. T.; Haertlein, M.; Maric, S.; Cárdenas, M. The production of matchout-deuterated cholesterol and the study of bilayer-cholesterol interactions. *Sci. Rep.* **2019**, *9* (1), 5118.
- (55) Lind, T. K.; Wacklin, H.; Schiller, J.; Moulin, M.; Haertlein, M.; Pomorski, T. G.; Cárdenas, M. Formation and characterization of supported lipid bilayers composed of hydrogenated and deuterated *Escherichia coli* lipids. *PLoS One* **2015**, *10* (12), No. e0144671.
- (56) Richards, M. J.; Hsia, C.-Y.; Singh, R. R.; Haider, H.; Kumpf, J.; Kawate, T.; Daniel, S. Membrane protein mobility and orientation preserved in supported bilayers created directly from cell plasma membrane blebs. *Langmuir* **2016**, *32* (12), 2963–2974.
- (57) Lind, T. K.; Skoda, M. W.; Cárdenas, M. Formation and characterization of supported lipid bilayers composed of phosphatidylethanolamine and phosphatidylglycerol by vesicle fusion, a simple but relevant model for bacterial membranes. *ACS Omega* **2019**, *4* (6), 10687–10694.
- (58) Montis, C.; Busatto, S.; Valle, F.; Zendrini, A.; Salvatore, A.; Gerelli, Y.; Berti, D.; Bergese, P. Biogenic supported lipid bilayers from nanosized extracellular vesicles. *Advanced Biosystems* **2018**, *2* (4), 1700200.
- (59) Cho, N.-J.; Cho, S.-J.; Cheong, K. H.; Glenn, J. S.; Frank, C. W. Employing an amphipathic viral peptide to create a lipid bilayer on Au and TiO₂. *J. Am. Chem. Soc.* **2007**, *129* (33), 10050–10051.
- (60) Hardy, G. J.; Nayak, R.; Alam, S. M.; Shapter, J. G.; Heinrich, F.; Zauscher, S. Biomimetic supported lipid bilayers with high cholesterol content formed by α -helical peptide-induced vesicle fusion. *J. Mater. Chem.* **2012**, *22* (37), 19506–19513.
- (61) Zan, G. H.; Jackman, J. A.; Cho, N.-J. AH peptide-mediated formation of charged planar lipid bilayers. *J. Phys. Chem. B* **2014**, *118* (13), 3616–3621.
- (62) Kim, M. C.; Gunnarsson, A.; Tabaei, S. R.; Höök, F.; Cho, N.-J. Supported lipid bilayer repair mediated by AH peptide. *Phys. Chem. Chem. Phys.* **2016**, *18* (4), 3040–3047.
- (63) Rädler, J.; Strey, H.; Sackmann, E. Phenomenology and kinetics of lipid bilayer spreading on hydrophilic surfaces. *Langmuir* **1995**, *11* (11), 4539–4548.
- (64) Nissen, J.; Jacobs, K.; Rädler, J. O. Interface dynamics of lipid membrane spreading on solid surfaces. *Phys. Rev. Lett.* **2001**, *86* (9), 1904–1907.
- (65) Sanii, B.; Parikh, A. N. Surface-energy dependent spreading of lipid monolayers and bilayers. *Soft Matter* **2007**, *3* (8), 974–977.
- (66) Sugihara, K.; Jang, B.; Schneider, M.; Vörös, J.; Zambelli, T. A universal method for planar lipid bilayer formation by freeze and thaw. *Soft Matter* **2012**, *8* (20), 5525–5531.
- (67) Szoka, F.; Papahadjopoulos, D. Procedure for preparation of liposomes with large internal aqueous space and high capture by reverse-phase evaporation. *Proc. Natl. Acad. Sci. U. S. A.* **1978**, *75* (9), 4194–4198.
- (68) Hohner, A. O.; David, M. P. C.; Rädler, J. O. Controlled solvent-exchange deposition of phospholipid membranes onto solid surfaces. *Biointerphases* **2010**, *5* (1), 1–8.
- (69) Tabaei, S. R.; Choi, J.-H.; Haw Zan, G.; Zhdanov, V. P.; Cho, N.-J. Solvent-assisted lipid bilayer formation on silicon dioxide and gold. *Langmuir* **2014**, *30* (34), 10363–10373.
- (70) Tabaei, S. R.; Jackman, J. A.; Kim, S.-O.; Zhdanov, V. P.; Cho, N.-J. Solvent-assisted lipid self-assembly at hydrophilic surfaces: Factors influencing the formation of supported membranes. *Langmuir* **2015**, *31* (10), 3125–3134.
- (71) Tabaei, S. R.; Jackman, J. A.; Kim, M.; Yorulmaz, S.; Vafaei, S.; Cho, N.-J. Biomembrane fabrication by the solvent-assisted lipid bilayer (SALB) method. *J. Visualized Exp.* **2015**, No. 106, No. e53073.
- (72) Ferhan, A. R.; Yoon, B. K.; Park, S.; Sut, T. N.; Chin, H.; Park, J. H.; Jackman, J. A.; Cho, N.-J. Solvent-assisted preparation of supported lipid bilayers. *Nat. Protoc.* **2019**, *14*, 2091–2118.
- (73) Kim, M. C.; Gillissen, J. J. J.; Tabaei, S. R.; Zhdanov, V. P.; Cho, N.-J. Spatiotemporal dynamics of solvent-assisted lipid bilayer formation. *Phys. Chem. Chem. Phys.* **2015**, *17* (46), 31145–31151.
- (74) Gillissen, J. J. J.; Tabaei, S. R.; Cho, N.-J. A phenomenological model of the solvent-assisted lipid bilayer formation method. *Phys. Chem. Chem. Phys.* **2016**, *18* (35), 24157–24163.

- (75) Chin, H.; Gillissen, J. J.; Miyako, E.; Cho, N.-J. Microfluidic liquid cell chamber for scanning probe microscopy measurement application. *Rev. Sci. Instrum.* **2019**, *90* (4), 046105.
- (76) Jackman, J. A.; Tabaei, S. R.; Zhao, Z.; Yorulmaz, S.; Cho, N.-J. Self-assembly formation of lipid bilayer coatings on bare aluminum oxide: overcoming the force of interfacial water. *ACS Appl. Mater. Interfaces* **2015**, *7* (1), 959–968.
- (77) Venkatesan, B. M.; Polans, J.; Comer, J.; Sridhar, S.; Wendell, D.; Aksimentiev, A.; Bashir, R. Lipid bilayer coated Al₂O₃ nanopore sensors: towards a hybrid biological solid-state nanopore. *Biomed. Microdevices* **2011**, *13* (4), 671–682.
- (78) Mager, M. D.; Almquist, B.; Melosh, N. A. Formation and characterization of fluid lipid bilayers on alumina. *Langmuir* **2008**, *24* (22), 12734–12737.
- (79) Tabaei, S. R.; Vafaei, S.; Cho, N.-J. Fabrication of charged membranes by the solvent-assisted lipid bilayer (SALB) formation method on SiO₂ and Al₂O₃. *Phys. Chem. Chem. Phys.* **2015**, *17* (17), 11546–11552.
- (80) Tabaei, S. R.; Ng, W. B.; Cho, S.-J.; Cho, N.-J. Controlling the formation of phospholipid monolayer, bilayer, and intact vesicle layer on graphene. *ACS Appl. Mater. Interfaces* **2016**, *8* (18), 11875–11880.
- (81) Su, H.; Liu, H.-Y.; Pappa, A.-M.; Hidalgo, T. C.; Cavassani, P.; Inal, S.; Owens, R. M.; Daniel, S. Facile generation of biomimetic-supported lipid bilayers on conducting polymer surfaces for membrane biosensing. *ACS Appl. Mater. Interfaces* **2019**, *11* (47), 43799–43810.
- (82) Losada-Pérez, P.; Polat, O.; Parikh, A. N.; Seker, E.; Renner, F. U. Engineering the interface between lipid membranes and nanoporous gold: A study by quartz crystal microbalance with dissipation monitoring. *Biointerphases* **2018**, *13* (1), 011002.
- (83) Yeagle, P. L. Cholesterol and the cell membrane. *Biochim. Biophys. Acta, Rev. Biomembr.* **1985**, *822* (3–4), 267–287.
- (84) McMullen, T. P.; Lewis, R. N.; McElhaney, R. N. Cholesterol-phospholipid interactions, the liquid-ordered phase and lipid rafts in model and biological membranes. *Curr. Opin. Colloid Interface Sci.* **2004**, *8* (6), 459–468.
- (85) Tabaei, S. R.; Jackman, J. A.; Kim, S.-O.; Liedberg, B.; Knoll, W.; Parikh, A. N.; Cho, N.-J. Formation of cholesterol-rich supported membranes using solvent-assisted lipid self-assembly. *Langmuir* **2014**, *30* (44), 13345–13352.
- (86) Radhakrishnan, A.; McConnell, H. M. Chemical activity of cholesterol in membranes. *Biochemistry* **2000**, *39* (28), 8119–8124.
- (87) Simonsson, L.; Höök, F. Formation and diffusivity characterization of supported lipid bilayers with complex lipid compositions. *Langmuir* **2012**, *28* (28), 10528–10533.
- (88) Kawakami, L. M.; Yoon, B. K.; Jackman, J. A.; Knoll, W.; Weiss, P. S.; Cho, N.-J. Understanding how sterols regulate membrane remodeling in supported lipid bilayers. *Langmuir* **2017**, *33* (51), 14756–14765.
- (89) Tabaei, S. R.; Jackman, J. A.; Liedberg, B.; Parikh, A. N.; Cho, N.-J. Observation of stripe superstructure in the β -two-phase coexistence region of cholesterol-phospholipid mixtures in supported membranes. *J. Am. Chem. Soc.* **2014**, *136* (49), 16962–16965.
- (90) Maekawa, T.; Chin, H.; Nyu, T.; Sut, T. N.; Ferhan, A. R.; Hayashi, T.; Cho, N.-J. Molecular diffusion and nano-mechanical properties of multi-phase supported lipid bilayers. *Phys. Chem. Chem. Phys.* **2019**, *21* (30), 16686–16693.
- (91) Mori, T.; Chin, H.; Kawashima, K.; Ngo, H. T.; Cho, N.-J.; Nakanishi, W.; Hill, J. P.; Ariga, K. Dynamic control of intramolecular rotation by tuning the surrounding two-dimensional matrix field. *ACS Nano* **2019**, *13* (2), 2410–2419.
- (92) Guo, J.; Ho, J. C. S.; Chin, H.; Mark, A. E.; Zhou, C.; Kjelleberg, S.; Liedberg, B.; Parikh, A. N.; Cho, N.-J.; Hinks, J.; Mu, Y.; Seviour, T. Response of microbial membranes to butanol: Interdigitation vs. disorder. *Phys. Chem. Chem. Phys.* **2019**, *21* (22), 11903–11915.
- (93) Tabaei, S. R.; Guo, F.; Rutaganira, F. U.; Vafaei, S.; Choong, I.; Shokat, K. M.; Glenn, J. S.; Cho, N.-J. Multistep compositional remodeling of supported lipid membranes by interfacially active phosphatidylinositol kinases. *Anal. Chem.* **2016**, *88* (10), 5042–5045.
- (94) Griebenow, K.; Klibanov, A. M. On protein denaturation in aqueous-organic mixtures but not in pure organic solvents. *J. Am. Chem. Soc.* **1996**, *118* (47), 11695–11700.
- (95) Diller, A.; Loudet, C.; Aussenac, F.; Raffard, G.; Fournier, S.; Laguerre, M.; Grélaud, A.; Opella, S. J.; Marassi, F. M.; Dufourc, E. J. Bicelles: a natural 'molecular goniometer' for structural, dynamical and topological studies of molecules in membranes. *Biochimie* **2009**, *91* (6), 744–751.
- (96) Dürr, U. H.; Gildenberg, M.; Ramamoorthy, A. The magic of bicelles lights up membrane protein structure. *Chem. Rev.* **2012**, *112* (11), 6054–6074.
- (97) Poulos, S.; Morgan, J. L.; Zimmer, J.; Faham, S. Bicelles coming of age: an empirical approach to bicelle crystallization. *Methods Enzymol.* **2015**, *557*, 393–416.
- (98) Glover, K. J.; Whiles, J. A.; Wu, G.; Yu, N.-j.; Deems, R.; Struppe, J. O.; Stark, R. E.; Komives, E. A.; Vold, R. R. Structural evaluation of phospholipid bicelles for solution-state studies of membrane-associated biomolecules. *Biophys. J.* **2001**, *81* (4), 2163–2171.
- (99) Beaugrand, M.; Arnold, A. A.; Ħnin, J. r. m.; Warschawski, D. E.; Williamson, P. T.; Marcotte, I. Lipid concentration and molar ratio boundaries for the use of isotropic bicelles. *Langmuir* **2014**, *30* (21), 6162–6170.
- (100) Mineev, K.; Nadezhdin, K.; Goncharuk, S.; Arseniev, A. Characterization of small isotropic bicelles with various compositions. *Langmuir* **2016**, *32* (26), 6624–6637.
- (101) Sut, T. N.; Jackman, J. A.; Yoon, B. K.; Park, S.; Kolahdouzan, K.; Ma, G. J.; Zhdanov, V. P.; Cho, N.-J. Influence of NaCl concentration on bicelle-mediated SLB formation. *Langmuir* **2019**, *35* (32), 10658–10666.
- (102) Zeineldin, R.; Last, J. A.; Slade, A. L.; Ista, L. K.; Bisong, P.; O'Brien, M. J.; Brueck, S. R. J.; Sasaki, D. Y.; Lopez, G. P. Using bicellar mixtures to form supported and suspended lipid bilayers on silicon chips. *Langmuir* **2006**, *22* (19), 8163–8168.
- (103) Tabaei, S. R.; Jönsson, P.; Brändén, M.; Höök, F. Self-assembly formation of multiple DNA-tethered lipid bilayers. *J. Struct. Biol.* **2009**, *168* (1), 200–206.
- (104) Morigaki, K.; Kimura, S.; Okada, K.; Kawasaki, T.; Kawasaki, K. Formation of substrate-supported membranes from mixtures of long- and short-chain phospholipids. *Langmuir* **2012**, *28* (25), 9649–9655.
- (105) Kolahdouzan, K.; Jackman, J. A.; Yoon, B. K.; Kim, M. C.; Johal, M. S.; Cho, N.-J. Optimizing the formation of supported lipid bilayers from bicellar mixtures. *Langmuir* **2017**, *33* (20), 5052–5064.
- (106) Sut, T. N.; Jackman, J. A.; Cho, N.-J. Understanding how membrane surface charge influences lipid bicelle adsorption onto oxide surfaces. *Langmuir* **2019**, *35* (25), 8436–8444.
- (107) Jackman, J. A.; Zan, G. H.; Zhao, Z.; Cho, N.-J. Contribution of the hydration force to vesicle adhesion on titanium oxide. *Langmuir* **2014**, *30* (19), 5368–5372.
- (108) Ferhan, A. R.; Špačková, B.; Jackman, J. A.; Ma, G. J.; Sut, T. N.; Homola, J.; Cho, N.-J. Nanoplasmonic ruler for measuring separation distance between supported lipid bilayers and oxide surfaces. *Anal. Chem.* **2018**, *90* (21), 12503–12511.
- (109) Sut, T. N.; Park, S.; Choe, Y.; Cho, N.-J. Characterizing the supported lipid membrane formation from cholesterol-rich bicelles. *Langmuir* **2019**, *35* (47), 15063–15070.
- (110) Rutaganira, F. U.; Fowler, M. L.; McPhail, J. A.; Gelman, M. A.; Nguyen, K.; Xiong, A.; Dornan, G. L.; Tavshanjian, B.; Glenn, J. S.; Shokat, K. M. Design and structural characterization of potent and selective inhibitors of phosphatidylinositol 4 kinase III β . *J. Med. Chem.* **2016**, *59* (5), 1830–1839.
- (111) Andersson, A. S.; Glasmästar, K.; Sutherland, D.; Lidberg, U.; Kasemo, B. Cell adhesion on supported lipid bilayers. *J. Biomed. Mater. Res., Part A* **2003**, *64* (4), 622–629.
- (112) Groves, J. T.; Dustin, M. L. Supported planar bilayers in studies on immune cell adhesion and communication. *J. Immunol. Methods* **2003**, *278* (1–2), 19–32.

(113) Vafaei, S.; Tabaei, S. R.; Biswas, K. H.; Groves, J. T.; Cho, N.-J. Dynamic cellular interactions with extracellular matrix triggered by biomechanical tuning of low-rigidity, supported lipid membranes. *Adv. Healthcare Mater.* **2017**, *6* (10), 1700243.

(114) Xia, Z.; Woods, A.; Quirk, A.; Burgess, I. J.; Lau, B. L. T. Interactions between polystyrene nanoparticles and supported lipid bilayers: Impact of charge and hydrophobicity modification by specific anions. *Environ. Sci.: Nano* **2019**, *6* (6), 1829–1837.